Molecular Crystals and Liquid Crystals

Publication details, including instructions for authors and subscription information:
http://www.tandfonline.com/loi/gmcl20

Charge Distribution Inside Thin Liquid Crystal Layer

Andrzej Walczak [a]

[a] Institute of Applied Physics MUT, Warsaw, Poland

Version of record first published: 18 Oct 2010

To cite this article: Andrzej Walczak (2004): Charge Distribution Inside Thin Liquid Crystal Layer, Molecular Crystals and Liquid Crystals, 409:1, 505-513

To link to this article: http://dx.doi.org/10.1080/15421400490434207

Mol. Cryst. Liq. Cryst., Vol. 409, pp. 505–513, 2004

ISSN: 1542-1406 print/1563-5287 online
DOI: 10.1080/15421400490434207

CHARGE DISTRIBUTION INSIDE THIN LIQUID CRYSTAL LAYER

*Andrzej Walczak**
Institute of Applied Physics MUT, 00-908 Warsaw, ul.Kaliskiego 2, Poland

We suppose that the phenomena of the light induced deformation in a thin liquid crystal (LC) layer depends strongly on light induced discharge on the boundary between substrate and the LC layer. It seems meaningful to find out what decides about the charge gathering and trapping near this boundary. The creation of the electric potential traps in this area has been explained. The shape of the electric field distribution inside liquid crystalline layer has been found to recognize way of mentioned traps formation. The exact, soliton like solution of the Ericksen-Leslie equation (EL equation) in an isotropic elasticity approximation has been demonstrated for this aim. The measurement of the refractive indices profile across the liquid crystal layer has been fitted to the solution of EL equation allowing one to determine electric field distribution inside the LC layer. The structure and origin of the charge trapping mentioned above has been shown in detail. Obtained results allow one to get conditions for a light induced discharge of the LC layer-substrate region.

Keywords: charge distribution; liquid crystal layer; photo-induced refraction

INTRODUCTION

It is well known since Janossy [1] that the presence of a dye in a nematic liquid crystal causes a decrease of the Frederick's threshold voltage. Even light of power of some 10^{-3} W/cm^2 allows one to achieve photo-induced deformation in a dye doped LC crystal. Simultaneous use of a DC driving electrical field make that range lower. After Janossy's work many excellent results has been established in the host-guest liquid crystalline systems [2].

Among them optically induced diffraction gratings and holograms in a dye-doped liquid crystal seems to be most promising [3]. The memory effect has been also described [4–6]. Duration of the memory effect

This work was sponsored by grant of MUT no. PBS 636.
*Corresponding author. E-mail: awalc@iar.wat.waw.pl

depends on a thickness of the isolating layer deposited onto conducting layer in a LC sandwich. It depends also on resistivity of the used LC sample [7]. Such observation seems to confirm that ionic current of a long duration is present in a LC sample.

The simulation of ion transport in the nematic liquid crystal displays (LCD) has been shown by Colpaert, Meyere, Verweire [8], and by Colpaert, and Maximus [9]. They explain the existence of a space charge limit (SCL) that can build up an internal electric field exactly opposite to the driving field. Naemura has shown that for mobility of ions estimated to be of the order of 10^{-8}–10^{-10} (m^2/V s) the flight time of the ions across the 5 μm gap should be equal to 0.5–50 ms [10]. This movement of ions is the origin of the electric conductance of the LC.

So if the AC driving field of frequency above approximately 1 kHz is applied then all carriers do not reach electrode during the cycle time. Below this frequency SCL presence should be taken into account during analyse of an electric field inside LC slab and above this frequency it may be neglected. At these lower frequencies ions take part in final deformation of the director field in LC. It is obvious that molecular ordering also influences current and charge behaviour. Such coupling of phenomena produces rather complicated and hard to resolve task. As far as the author is aware it is not resolved in general yet.

Charge carriers in LC slab are considered to be ions, which are partly dissolved from the peripheral materials and partly generated by a dielectric dissociation in the LC materials. The number of the ions may be affected by driving field or by incident light. The ions are stabilised in form of hydrated or solvated ions with water and other polar molecules such as the solvent [11]. Some authors suggest that ions may be trapped on the LC-substrate boundary and induce a residual DC potential which remains for longer time than the polarization induced residual DC (see [10]). It seems to be possible but hard to measure and prove. Some authors suggest, on the other hand, that DC usage results in non-symmetric charge distribution in LC slab [12]. Both suggestions should be explained in terms of electric potential variation across the LC slab.

As a resume of an actual state of art one can say that during AC field interaction in the LC layer all charges move with the AC driving field frequency. In thick enough LC layer charges do not access the electrodes. We can estimate that the oscillating movement of the ions is of amplitude less than 0.1 micrometer for large enough frequency of the driving field. Following Naemura (see [9]) it should be achieved at frequencies over 500 kHz. When an external illumination is added then some assembled charge may be generated and local charge balance as well as electric field distribution may vary. The most important information we need to know seems to be the connection between the light intensity or frequency and

an internal field variation. This connection remains with no efficient theoretical model and explanation.

In such situation the electric field distribution inside LC layer is an important step or tool to analyse experimental data. Such distribution has been be described here as well as some experimental results. The main assumptions and ideas are: the driving field has been applied as DC signal followed after some time by an AC component; the DC maintains the steady charge distribution and trapping on the LC-substrate boundary; the frequency of AC component is high enough to neglect the SLC; the charge q is created near the LC-substrate boundary by means of illumination say. Such assumptions give us conditions of simulation of the electric filed inside LC layer.

THEORY AND ASSISTED EXPERIMENT

To simplify the theoretical model let us assume an isotropic elasticity approximation in the LC. With such an assumption the Ericksen-Leslie equation has the form [13]:

$$\varphi_{zz} = -\frac{\varepsilon_0 \Delta\varepsilon E^2}{2K_F} \sin 2\varphi(z) \tag{1}$$

It is one of the differential equations of the kind [14]:

$$y_{zz} = cf(y) \tag{2}$$

The coefficient before sine in (1) has been denoted as c. Simple integration gives:

$$\frac{dy}{dz} = \pm\sqrt{2c\int f(y) + C_1} \tag{3}$$

When symmetric planar LC layer is deformed then the condition like in formula (4) has to be fulfilled in the middle of the layer and C_1 can be set equal to null.

$$\left(\frac{dy}{dz}\right)^2 = 0 \tag{4}$$

Finally the exact analytical solution of EL equation is like below:

$$\varphi(z) = 2ArcTan\left[Exp\left(\sqrt{\frac{\varepsilon_0 \Delta\varepsilon E^2}{K_F}}\right)(\pm z + C_2)\right] \tag{5}$$

The full solution of EL in the LC layer is the sum of both integrals exhibited in (5). It is soliton like solution of the EL equation. As time independent it describes a "frozen" soliton. In formula (5) an angle ϕ is measured from the normal direction in reference to LC layer. If hard anchoring ($\phi = \pi/2$ at $z = \pm d/2$) is imposed then $C_2 = d/2$. Other terms in (5) denote as follows K_F–Frank elastic constant, ε_0–dielectric constant, $\Delta\varepsilon$ – dielectric constant anisotropy, E – electric field amplitude. As we know an electric field E in the equation EL (see formula 1), and so in form (5), is the local value of the field inside LC layer, at the point of differentiation. This value is generally unknown. It depends on the external field value and on the dielectric properties of the LC.

The formula (5) describes the optical axis distribution inside the LC layer. So if we manage to measure this distribution we obtain possibility to determine $E(z)$. The refraction index profile measurement across the LC layer is the way to do it. A method for this measurement has been developed earlier so only main features will be described here to explain the concerned phenomenon [15].

The guided wave called mode in the waveguide (see Fig. 1) is excited only in the case of equality between measured propagation constant of one of the possible mode's and the incident wave vector projection onto waveguide plane [16]. In fact such mode is a wave, which propagates along waveguide but remains standing wave in the direction transverse

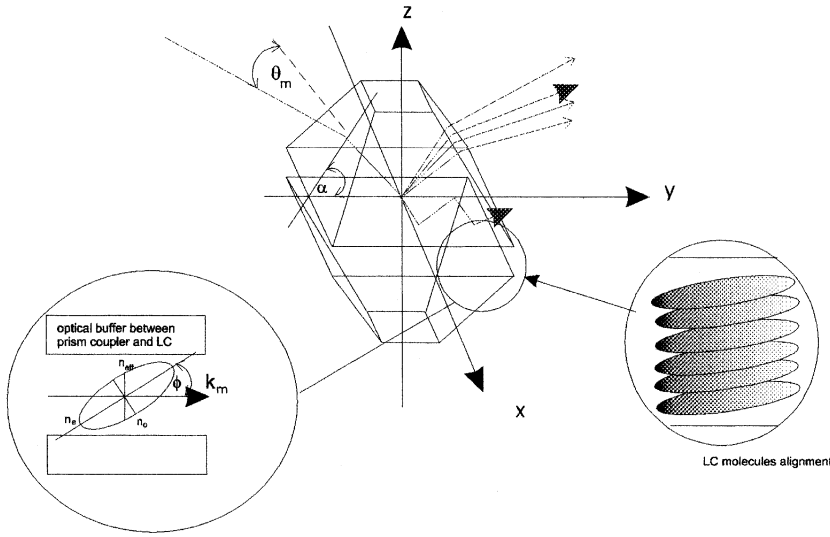

FIGURE 1 Scheme of the idea of a prism coupler method applied with LC waveguide.

to propagation. The standing wave arises between two turning points say z_m. That standing wave undergoes internal reflection in turning points with the phase change described by Fresnel rules [17]. The general rule must be fulfilled:

$$\frac{2\pi}{\lambda}\int_{-z_m}^{z_m}\left(n(z)^2 - N2\,m\right)^{1/2}dz + 2\phi_{ref} = 2\pi m \tag{6}$$

The $(2\pi/\lambda)\,Nm$ in (6) is the propagation constant of the guided wave, and m is the mode consecutive number while ϕ_{ref} is phase variation during internal reflection of the guided mode. In the prism coupler method applied in LC waveguide the guided modes propagation constant has been measured (see Fig. 1) as:

$$N_m = n_{eff}\frac{\omega}{c} = n_p \sin\left(\alpha + arc\sin\left(\frac{\sin(\theta_m)}{n_p}\right)\right) \tag{7}$$

In (7) α is prism' angle and θ_m is an incident angle for waveguide mode excitation. The n_p item means the refraction index of coupling prism. The wave number in free space is equal to ω/c. Both angles, α and θ_m, are easily measured. So N_m can be obtained from measurements. For known N_m the localization of the turning points z_m in the waveguide cross-section as well as $n(z_m)$ values can be obtained from the formula (6). It is easy to see that measurement of N_m family for the observed waveguide modes is enough to obtain turning points position as well as $n(z)$ form finally. In fact (see Fig. 1) $n(z)$ is equivalent to $n_{eff}(z)$, which is seeing by each mode between its turning points. A known formula describes the effective refraction index:

$$n_{eff} = \frac{n_o n_e}{\sqrt{n_o^2 Sin^2\,\phi(E,z) + n_e^2 Cos^2\,\phi(E,z)}} \tag{8}$$

Value E in (8) is local value of the driving field in point z while angle ϕ can be described by formula (5). By fitting measured n_{eff} in turning points of the guided modes shown in Figure 2 one can obtain values of E in those points.

Values of the refractive index in a discrete set of the mode's turning points are as in Figure 2 [18]. It has been determined in the $3\,\mu$m thick NL waveguide of 6CHBT (4-trans-4-n-hexyl-cyclohexyl-isothiocyanatobenzene). These values are applied further for determination of the local electric field in turning points.

The optic buffer between prism and the LC layer in Figure 1 consists of polyimide/SiO_2/ITO-stacked layers thick enough to guarantee guided modes existence.

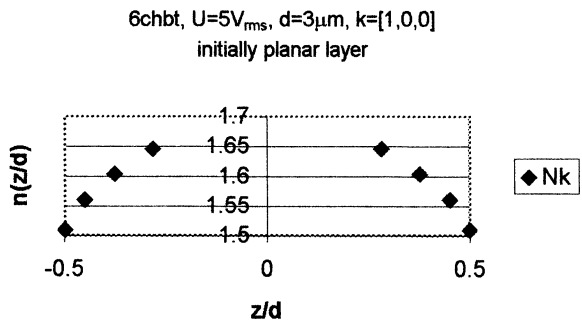

FIGURE 2 Refractive index profile $n(z_k)$ in turning points z_k obtained in 6CHBT tuned waveguide for 5 V driving electric field at frequency equal to 200 kHz (k means the wave vector direction as in Figure 1 and d is layer thickness).

FIELD INSIDE LC LAYER

As fitting procedure of the measured $n_{eff}(z_m)$ and soliton-like solution (5) has been done then the electric field shape across the 6CHBT layer is like in Figure 3. The obtained electric field distribution contains components from all charges in the LC layer volume and on the LC-substrate boundary. Local illumination disturbs exactly this charge first of all. The relation between an illumination and a generated charge remains generally unknown. Nevertheless we can assume that it is always present as well as that illumination generates constrained value of a localised charge.

The presence of the localised photo-induced charge in the LC-substrate boundary vicinity produces the polarising charge distributed immediately at the boundary. Description of that charge in analysed case is shown in formula (9)

$$\sigma_{pol} = -\frac{q}{2\pi}\frac{\varepsilon_{AL} - \varepsilon_{eff}}{\varepsilon_{eff}(\varepsilon_{AL} + \varepsilon_{eff})}\frac{d_g}{\left(\rho^2 + d_g^2\right)^{3/2}} \tag{9}$$

The ε_{AL} is dielectric permittivity of the aligning layer, ε_{eff} is the effective dielectric permittivity of the 6CHBT here calculated with the use of angle described by (5), d_g is the induced charge layer thickness, and q is the value of the induced charge. The distance ρ is measured in plane of the layer. In further calculation the q has been arbitrary chosen as its value is generally unknown.

Both light-induced q and polarising charges σ are sources of electrostatic field. It should be added to the electric field created inside driven LC layer and shown in Figure 3. Finally shape of the potential in the cross-section of the LC layer is presented in Figure 4 as a sum of all components: internal

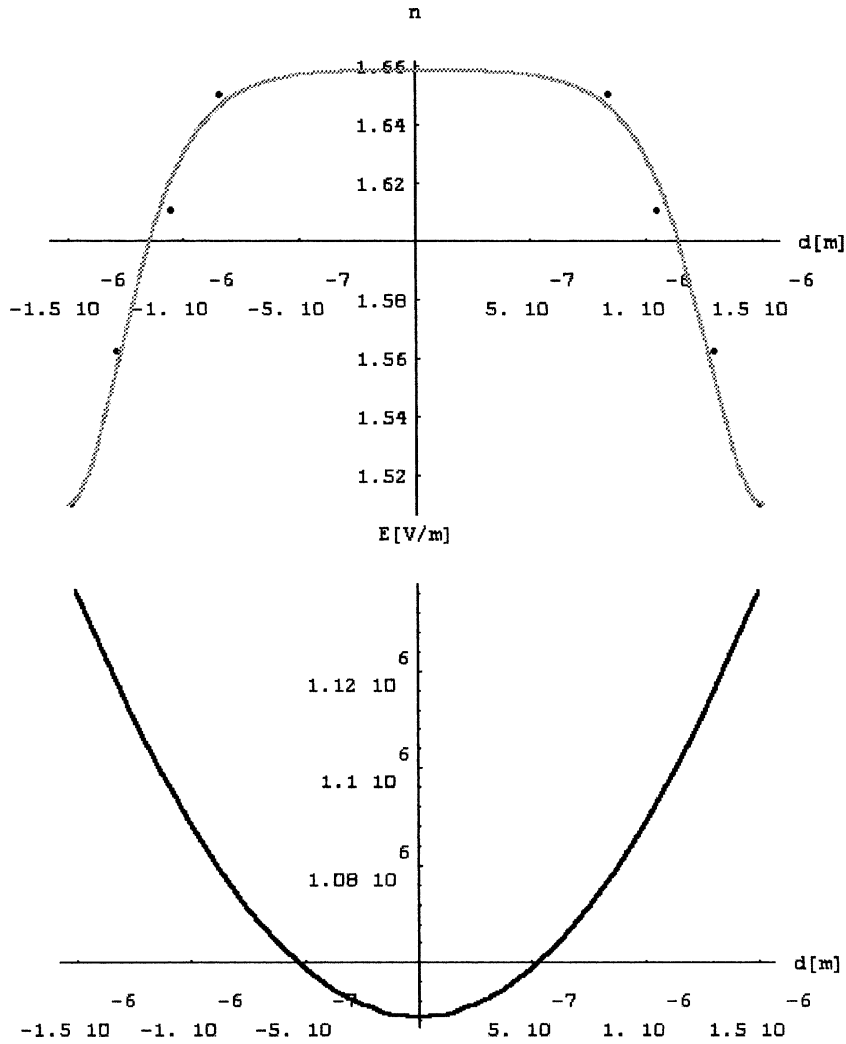

FIGURE 3 The fitting outcome (upper side) and obtained electric field shape (lower side) across the 6CHBT layer at 5 V high frequency external driving field. The dots in upper side mean the same as in Figure 2.

electric field created by dipoles in the LC layer, photo-induced charge and polarising charge. One can see that near LC-substrate boundary the potential valley exists. It may be explanation for charge trapping in that region of the LC device. It explains also long lasting deformation of the director field observed as memory effect.

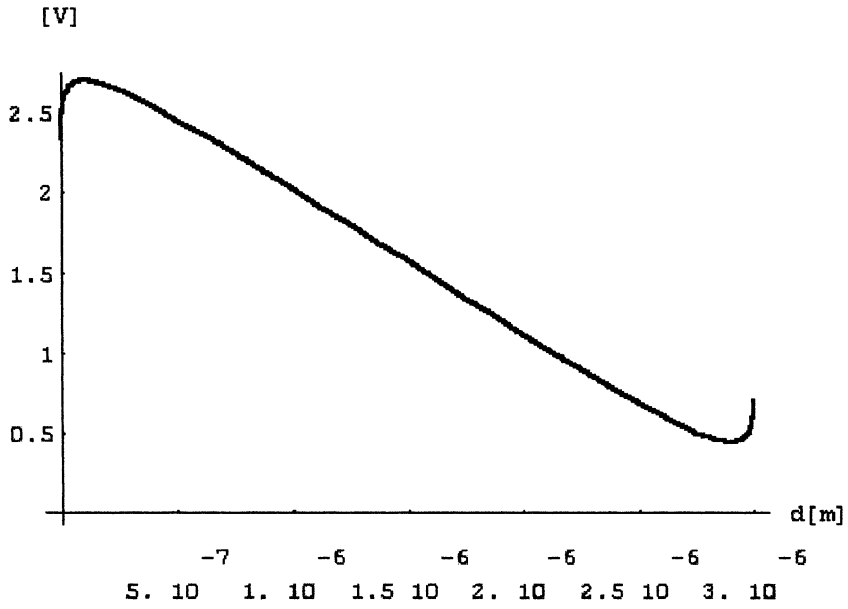

FIGURE 4 Final shape of the potential across the 6CHBT layer when driven by 5 V external voltage. Assumed concentration of photo-induced carrier equal to $10^{16}/\text{cm}^3$.

Electrostatic potential caused by all boundary charges has been simulated numerically and added to the obtained potential of the internal field from charges inside the LC layer presented in Figure 3.

To obtain such a shape the existence of DC signal must be assumed to divide positive and negative carriers. That assumption provides two differently oriented extremes seen in the Figure 4. Each extreme creates the trap for opposite carriers. On the other hand, the DC signal gives the double charge layer on the each boundary with sum of all carriers equal to zero. If the light induced charge q raises it causes the near surface polarisation and the results described above.

CONCLUSIONS

It has been shown that in presence of a DC bias-driving field in the LC device the photo-induced charge in the LC-substrate boundary vicinity can produce a potential trap. Such traps can be bounds for the charge carriers. When the AC field is the only component of driving signal then photo-induced charge as well as other free carriers contaminated the LC

material remains neutral, as it is cloud of opposite carriers assembled in a constrained area. The DC signal causes carriers distribution.

Obtained extremes in the potential distribution depend on the carrier concentration and dielectric permittivity of the aligning layer and the LC (see formula (9)). So joined presence of a DC signal and the illumination of the LC layer can cause phenomena of charge trapping on the LC-substrate boundary.

The presence of the electric potential extremes explains the long lasting carrier presence in the illuminated LC devices. This extremes are localized near surface between LC and the substrate. Such an explanation has not been presented earlier and is new to some extent.

The filed shape inside LC layer has been obtained with the aid of soliton – like solution of EL equation and an exploited experiment for refractive indices profile measurement. As far as authors knew it is the first picture of the electric field distribution inside LC layer. Here it has been obtained when driving field is a sum of DC and AC signals.

REFERENCES

[1] Janossy, I. & Lloyd, A. D. (1991). *Mol. Cryst. Liq. Cryst.*, *203*, 77–84.
[2] Macdonald, R., Meindl, P., Chilaya, G., & Sikharulidze, D. (1998). *Mol. Cryst. Liq. Cryst.*, *320*, 115–126.
[3] Chen, A. G. & Brady, D. J. (1992). *Optics Lett.*, *17*, 441–445.
[4] Sun, S. T., Gibbons, W. M., & Shannon, P. J. (1994). *Liquid Crystals*, *12*, 869–874,(1992); also Mol. Cryst. Liq. Cryst., *251*, 191–197.
[5] Marusii, T., Reznikov, Yu., & Voloshchenko, D. (1994). *Mol. Cryst. Liq. Cryst.*, *251*, 209–217.
[6] Slussarenko, S., Francescangeli, O., Simoni, F., & Reznikov, Yu. (1997). *App. Phys. Lett*, *71*, 3313–3320.
[7] Parka, J. "*Własności elektrooptyczne i zastosowanie nematycznych ciekłych kryształów domieszkowanych barwnikami dichroicznymi*", (Warszawa, WAT, 2001) 104, Figure 5.12, in Polish
[8] Colpaert, C., Meyere, A. D., & Verweire, B. (1996). *Euro Display*, *P-32*, 325–329.
[9] Colpaert, C. & Maximus, B. (1995). *SID 95 Digest*, 609–612.
[10] Naemura, S. (2000). *Journal of the SID*, *8/1*, 5–9.
[11] Bremer, M. & Naemura, S. (1998). *Jpn. J. Appl. Phys.*, *L88–90*, 37.
[12] Macdonald, R., Meindl, P., Busch, S., & Eichler, H. J. (1998). *SPIE Proc.*, *3745*, 134–142.
[13] Iam-Choon Khoo, & Shin-Tson Wu, (1993). "*Optics and Nonlinear Optics of Liquid Crystals*", (World Scientific Publisher: Singapore), 161.
[14] Walczak, A. (2002). *Opto-Electronics Review*, *10*, 1, 43.
[15] Walczak, A. (1998). *Acta. Physica. Polonica.*, *94*, 5–6, 803.
[16] Tien, P. K. (1971). *Appl. Optics*, *10*, 11, 2395.
[17] Kersten, R. Th. (1975). *Optica. Acta.*, *22*, 6, 503.
[18] Walczak, A. (1998). *Opto-Electronics Review*, *6*, 4, 263.